Investigation of Ergodic Character of Quantized Vibrational Motion†

Andreas Bäck,* Sture Nordholm, and Gunnar Nyman

Department of Chemistry, Physical Chemistry, Göteborg University, SE-412 96 Göteborg, Sweden

Received: February 27, 2004; In Final Form: May 26, 2004

The concept of quantum ergodicity and the degree of ergodic behavior reflected by the bound energy eigenstates are studied for some vibrational systems in two and three dimensions. Different approaches are attempted in order to be able to classify and quantify ergodicity in a given system by investigating the energy eigenfunctions. It is argued that the concept of quantum ergodicity is fundamentally connected to the similarity between eigenstates close in energy and to their globality. Previous investigations and definitions of quantum ergodicity can be seen to connect to this theme; they provide different measures of similarity between eigenstates. Here we propose two practical measures to investigate quantum ergodicity. The systems treated include the famous two-dimensional Henon-Heiles and Barbanis systems, which have previously been investigated both classically and quantum mechanically. As a more realistic three-dimensional example, we consider the vibrations of nonrotating NO_2 close to dissociation.

1. Introduction

In this report, we will address the question of the definition of quantum ergodicity and its relation to the classical concept and to applications such as unimolecular reactions. Specifically, we will relate the extent of ergodicity in a quantum system to the behavior of its energy eigenstates, which provides a more fundamental view of the concept as compared to the statistical analysis of eigenvalues used today for a wide variety of systems.

The concept of ergodicity is, together with the time scale under which ergodic relaxation takes place, one of the corner stones in modern theories of unimolecular reactions. The calculation of unimolecular rate constants via the statistical RRKM theory[1,2] assumes fully ergodic relaxation of the vibrational dynamics after the (collisional) activation of the reactant molecule and also that the relaxation is fast compared to the time scale of the reaction. However, for many reactions, especially over low reaction barriers, this assumption can certainly be questioned, and many attempts have been made to develop models which account for an incomplete ergodic relaxation at a finite rate.[3−8] Also, internal vibrational redistribution and thus mode-selective chemistry relates to the time scale on which a system may show ergodic behavior. It is further interesting to note that chaotic dynamics (which is ergodic) does not prevent coherent control.[9] Finally, the ergodic properties of quantum mechanical systems are of fundamental importance for the foundations of statistical mechanics and its many implementations in the form of simulation methods relying on the ergodic hypothesis which claims that time averages equal ensemble averages.

We begin by briefly reviewing previous suggestions that have been put forward as ways of analyzing quantum systems with respect to ergodicity. The first to discuss quantum ergodicity in the literature was apparently von Neumann.[10,11] He suggested that if the time averaged expectation value of any operator equals the average over phases in the (complex) expansion coefficients of the spectral basis then the system is quantum ergodic. This statement is to hold for any wave function of the system, but a simple analysis shows that this is equivalent to saying that a quantum system is ergodic if and only if its eigenvalue spectrum is nondegenerate. However, it is clear that quantum ergodicity must have a deeper meaning in order to match the content and relevance of the classical concept; a separable two-dimensional harmonic oscillator with incommensurate frequencies has no degenerate levels in its spectrum while being a clearly nonergodic system. Yet the fact that ergodic properties are somehow reflected in the spectrum of the system is to be expected. It was in nuclear physics that the interest in the statistical distribution of energy levels was initiated. A review of these developments is given by Porter,[12] and this book contains many of the early papers, notably by Wigner, who made important contributions. In short, it was found that there is a repulsion between neighboring energy levels if the dynamics is fully coupled (ergodic), whereas a system composed of several independent parts will tend toward a Poisson like distribution, where the energy levels are uncorrelated.

The interest in ergodic manifestations of spectra was introduced to chemistry by Percival,[13] Pomphrey,[14] and by Nordholm and Rice.[15] Although Nordholm and Rice discussed the expected regularization of energy level spacing that accompanies ergodicity, the main statement of this work was that the eigenstates themselves should contain more fundamental information about the ergodic properties of the system. Following this, they investigated the overlap properties of the eigenstates with suitable basis states and related a spread in this overlap over basis states of the same zeroth order energy to an ergodic behavior. This study concerned bound states, but in a following work,[16] also quasibound states were investigated, bringing the concept closer to unimolecular decay theory. Here the imaginary part of the eigenvalue, which is connected to the lifetime of the state, was compared for the states and large fluctuations in these give large variations in dissociation rates and hence a nonergodic behavior.

Berry[17] discussed classical approximations to the smoothed Wigner phase space distribution[18] of eigenfunctions for integrable and ergodic cases, paying special attention to the spatial

† Part of the "Gert D. Billing Memorial Issue".

* To whom correspondence should be addressed. E-mail: back@phc.gu.se.

10.1021/jp049113l CCC: $27.50
Published on Web 07/21/2004

behavior near the classical turning points. Furthermore, Berry conjectured that an ergodic eigenfunction looks like a Gaussian random function, which follows if it locally behaves like an isotropic random superposition of de Broglie waves. The investigations of Berry were tested numerically for stadium billiard systems by McDonald and Kaufman.[19] Unavoidable nonergodicity for quantum systems with symmetries causing degeneracies was pointed out by Heller,[20] but it was also noted by Kosloff and Rice[21] that the effect of the measuring process in quantum mechanics may reduce the impact of such nonclassical effects.

The nodal structure of ergodic/nonergodic eigenstates was discussed by Stratt et al,[22] where an irregular nodal pattern was related to ergodic states and a regular, ordered, pattern which assigns quantum numbers in different directions characterized nonergodic states. They also discussed the power spectra of energy eigenstates as an indication of ergodicity as well as suggested an improvement of the Nordholm−Rice method[15] based on the use of natural orbitals. Hutchinson and Wyatt[23] calculated the Wigner phase space distribution[18] on a Poincaré surface of section and compared it with results from classical trajectories. They obtained the expected trend toward more ergodic distributions as energy increased. Close agreement between wave functions and classical states in phase space was also found by Kay[24] within a time-dependent approach. An interesting discussion of the effect of the nature of the initial state preparation upon observation of ergodic behavior took place between Davis, Stechel, and Heller on one side and Brumer and Shapiro on the other.[25]

By assuming that, for ergodic cases, the spatial pattern of bound state eigenfunctions of approximately the same energy look roughly the same (close to the classical microcanonical density at that energy) Pechukas[26] managed, in the semiclassical limit, to derive the correct statistical distribution of energy levels showing the postulated level repulsion. Feit and Fleck[27] performed wave packet propagation and measured quantum chaos in terms of the decay of the autocorrelation function and the increase of uncertainty in coordinates and momenta. In an important paper,[28] Heller observed the phenomenon of scarring in wave functions of the classically chaotic stadium billiard system. These scars are an increase of probability density near the periodic classical orbits. Peres, Feingold, and Moiseyev[29] addressed the question of the classical limit of quantum chaos and observed how certain quantum expectation values for the energy eigenstates were related to the corresponding classical phase space average.

A measure of quantum ergodicity that is close to the classical concept was developed and investigated by Kay and Ramachandran.[30] The classical correlation between functions on phase space, which determine if the system is ergodic, was taken to the quantum regime by replacement of phase space functions with quantum mechanical traces of the corresponding operators. Billing and Jolicard[31] used adiabatic switching to see how (zeroth order) eigenstates loose memory about the initial separable situation as an anharmonic coupling is turned on slowly in time. Close in spirit to the early suggestion of Nordholm and Rice is the work of Benet et al[32] where they investigate the engagement of zeroth order states in the full Hamiltonian within a perturbational approach. De Polavieja, Borondo, and Benito[33] used Husimi functions to transform quantum mechanics to phase space and in this way found clear localization properties (nonergodicity) of eigenstates in a classically chaotic system. Kaplan and Heller and Zelditch[34] discussed what they call weak quantum ergodicity which, in contrast to Gaussian random eigenstates and random matrix theory, relaxes the demand on the eigenstates by investigating them only with smooth operators. Aurich et al[35] analyzed the maximum norm (L^∞) of eigenstates for various billiard systems. The growth of maximum norm in configuration space with energy, as well as the distribution of maximum amplitude inside the billiard provide information about ergodicity.

It must be emphasized that this introduction by no means gives a full account of all developments in the vast field of quantum ergodicity, but it serves nonetheless as a starting point for the following discussions. We shall return to some of these studies and discuss them in more detail later in this paper.

2. Theory

2.1. Classical Ergodicity and Unimolecular Reactions. Within the confines of classical mechanics the concept of ergodicity is clear and undisputed. It is also of obvious utility. Classical molecular dynamics is with few exceptions studied by trajectory calculations. A trajectory is a nonstatistical pure state of the classical system evolving on an energy surface of dimension one less than the full dimension of the classical system. The concept of ergodicity deals with the qualitative nature of the dynamics on the energy surface. The trajectory is a one-dimensional sequence of pure phase space states, $\Gamma(t)$, located on an energy surface. An ergodic system is defined to have trajectories such that they cover the energy surface uniformly; that is, each measurable subsurface on the energy surface is visited in proportion to its "area". Any classical physical property $A[\Gamma]$ then evolves in time so as to satisfy the ergodic hypothesis which says that the long time trajectory average of A equals its corresponding microcanonical average $\langle A\rangle_E$ for all but a set of initial trajectories of measure zero. This means that we have

$$\lim_{T\to\infty}\frac{1}{T}\int_0^T \mathrm{d}t\, A[\Gamma(t;\Gamma_0)] = \langle A\rangle_E \quad \text{for } E = H[\Gamma_0] \qquad (1)$$

Through the work of Birkhoff,[11,36] we know that if the system is nonergodic at the chosen energy E then the trajectory will span a subsurface which it samples uniformly and the entire energy surface is dynamically decomposable into subsurfaces without dynamical connections. The satisfaction of the ergodic hypothesis is often assumed, sometimes only implicitly, in the use of classical molecular dynamics to study the internal motions of molecules and fluids. This then allows the calculation of microcanonical property averages by the convenient trajectory method with its appealing dynamical character and often high numerical efficiency. In reality, there is a question of whether the system actually is ergodic. This focuses attention on the issue of the measure of ergodicity, which we shall consider here in the case of quantum dynamics. Also in the study of chemical reaction rates, particularly unimolecular reaction rates, the question of ergodicity plays a central role. The old RRK theory assumed complete ergodicity and an internal vibrational energy redistribution rate which is much faster than the isolated molecule reaction rates at the relevant energies. This assumption was taken over by the modern RRKM theories.[1,2] It is clear, however, from the early work of Slater,[3] who created a harmonic theory of unimolecular reactions based on essentially complete nonergodicity, that this assumption is not at all justified in general although it may well serve as a good approximation in many cases. Recently Leitner and Wolynes[7] and ourselves[8] have suggested that reality must be expected to fall somewhere between the Slater and RRKM assumptions showing incomplete ergodicity and perhaps internal vibrational redistribution rates

which are comparable or even slower than the isolated molecule decay rates at relevant energies. For these reasons, we must clearly extend the concept of ergodicity to quantum dynamics which applies far more accurately to the molecular vibrations in particular.

In our attempt to resolve the meaning and the measure of quantum ergodicity, we shall be guided by the classical concept of ergodicity with its proven relevance for relaxation phenomena and reaction rates. The correspondence principle suggests that we should be able to gain considerable insight by insisting that the concept and measure of quantum ergodicity we propose and explore here approach the correct classical limit. Nevertheless, we face an immediate contradiction. The classical concept deals with the way a trajectory samples a surface of equal energy states. In the quantum case, we will not have such an energy surface. There may be a set of degenerate eigenstates for a given energy level but quantum dynamics explicitly prohibits the flow of probability between such degenerate energy eigenstates and between any energy eigenstates. Thus, it would at first appear as if a system showing degenerate energy levels would automatically be nonergodic, whereas a system with nondegenerate energy eigenstates would be trivially ergodic. This view was indeed taken by von Neuman,[10,11] but it would rob the concept of quantum ergodicity of all its relevance. Thus, we must consider the nature of each quantum eigenstate to decide whether it is ergodic and to what degree. We must also recall that eigenstates are stationary states. To see dynamics, we must go to wave packets which are superpositions of many energy eigenstates and recall that the nature of the motion of a wave packet is related to both the energy eigenvalues and to the physical nature of the energy eigenstates, which describe the final distribution toward which the system relaxes.

2.2. Quantum Ergodicity and Its Relation to Energy Eigenstates. At the outset of this work,[37] it was noted that quantum ergodicity was very closely related to the similarity of eigenstates of nearly the same energy. Only then would a preparation of any initial state include all eigenstates within its energy dispersion in a "democratic" (maximally distributed) way, rather than risk that only a subset of the energy eigenstates, sharing some common feature with the initial state, excludes other subsets with other properties. As it turned out there existed already since 1974 a theorem for classically ergodic billiard systems by Shnirelman,[38,39] proving that in the semiclassical limit the eigenstates of the billiard system are uniformized in configuration space and that expectation values of pseudodifferential (phase space) operators go to their classical microcanonical average for almost all states. In a way, this means that the states in a sufficiently small energy interval become equal in the "test-space of smooth pseudo-differential operators". This certainly supports the suggested equivalence between quantum ergodicity and similarity between energy eigenstates, which is then assumed to hold approximately for real systems with potential and finite value of $\hbar$. Thus, complete ergodicity in an energy range will mean that the form of the energy eigenfunctions will change smoothly with energy. Rapid and random change between neighboring eigenfunctions will be a reliable sign of nonergodicity.

In line with the Shnirelman theorem, some of the studies mentioned in the Introduction[29,30,34] investigate quantum ergodicity in terms of the behavior of suitable sets of operators, which give a coarse grained investigation of similarity in phase space, where the exact features probed depend on the restrictions on the operators. Outside the semiclassical billiard regime defined by Shnirelman, the set of operators and the degree of similarity required will have to be properly relaxed.

Instead of discussing expectation values of operators one can at a more fundamental level discuss the globality of eigenstates,[15,22,32] where an ergodic state must be global (maximally delocalized) in all relevant basis sets. Two neighboring global energy eigenfunctions must be similar since the difference only arises from the small energy difference. The globality also implies similarity in a way very close to the idea of democratic participation of eigenstates in any initial state, since this of course also means initial states that are precisely the basis states of interest. In this way, similarity is an immediate consequence of globality of eigenstates in a given range of energy. Furthermore, detailed knowledge of the globality (i.e., the distribution of expansion coefficients) in basis functions that are eigenstates of an operator naturally contains richer information than just the expectation value of the operator (through all higher moments). Thus, globality is on equal footing with the Shnirelman suggestion of probing eigenstates through expectation values.

In time-dependent quantum dynamics, we find the real motivation for the interest in ergodicity. We want to know the qualitative behavior of the system, just as in the classical case (section 2.1), and the division of phase space, reflected by the ergodicity of the system, is clearly one of the fundamental properties of the general dynamics. For a time-independent Hamiltonian, the entire time development is known through the energy eigenstates, their energies, and the initial condition in form of the expansion coefficients at $t = 0$ via the spectral expression of time-dependence:

$$\Psi(t) = \sum_n a_n \exp(-iE_n t/\hbar)\psi_n \qquad (2)$$

This motivates the study of the energy eigenstates alone when the question of ergodicity is addressed. If we choose an initial $\Psi(0)$ (often a Gaussian wave packet, or some other physically interesting state), we obtain the expansion coefficients through $a_n = \langle\Psi(0)|\psi_n\rangle$, and the subsequent time evolution will forever be colored by this results. It is precisely therefore we must demand, in the case of ergodic dynamics, that these overlaps are democratic so that no particular class of initial states consequently prefers overlap with some subset of the ψ_n's. This subset then, must have some particular property (e.g., a different spatial probability distribution as in Figures 5−7) that the complementary subset lack, or otherwise there would have been no reason for the differences in overlap in the first place. This property will then for all times be reflected in the dynamics, due to the particular choice of initial state. Another initial state would in turn show another set of properties, making the overall system behavior dependent on initial preparation, which correspond exactly to classical nonergodic behavior. The democratic overlap of the energy eigenstates with (almost) any initial state is precisely the demand of similarity (or globality as mentioned previously), i.e., a set of eigenstates where no state stands out causing it to induce a particular type of dynamics. Clearly, the democratic overlap discussed above is limited by the energy of the initial state relative to the energy of the eigenstates. This energy criteria for the eigenstates depend on the exact energy dispersion of the initial state, and correspond to energy surfaces in the semiclassical limit where there are numerous states in a very small energy interval.

In eq 2, not only the eigenfunctions appear but also their energies. The energies present themselves as angular velocities of the phase of the time-dependent expansion coefficients and

relate directly to relaxation rates. We have already mentioned in the Introduction that in an ergodic system the energy levels will tend to repel each other, and this avoidance of near degeneracies will give a proper dephasing of the states. The repulsive character of the levels is demonstrated in the semiclassical limit by Pechukas,[26] where he obtains the statistics of regular eigenvalue spacings for ergodic systems by assuming the spatial similarity of bound eigenstates of nearly the same energy. The precise level spacing statistics obtained is called the Wigner distribution (not to be confused with the Wigner transform of wave functions into phase space distributions[18]) and is given by $p(S) = (\pi/2)S \exp(-\pi S^2/4)$, where S is the normalized spacing between two adjacent levels, $\Delta E/\langle \Delta E \rangle$. Thus, we see that the probability for zero spacing (degeneracy) between two levels is zero, and there is a peak probability at somewhat less than the average level spacing. In other words, the nowadays very popular investigations of energy level distributions, performed for a great variety of systems to elucidate the chaotic behavior of quantum systems, follows from the fact that eigenfunctions in an ergodic system must be similar, i.e., continuously varying with energy. If the states are not similar in this sense, they are instead independent and generate a random distribution of energy levels, where the position of a level does not depend on the position of nearby levels, hence, resulting in a Poisson type distribution.

The eigenvalue statistics for ergodic systems above demanded similarity in configuration space, but in passing, Pechukas also mentions an expected similarity of the Wigner phase space distribution[18] of the eigenstates, as first suggested by Nordholm and Rice[15] and by Berry,[17] and investigated numerically by Hutchinson and Wyatt[23] for the Henon-Heiles system. The suggestion is that, just as in the classical phase space of an ergodic system, a state in the quantum case should in the semiclassical limit uniformly cover the proper energy surface when Wigner transformed to phase space. Since the Wigner transform contains all possible information about the state, this is clearly the same as saying that eigenstates very close in energy are almost equal, which should hold approximately also when we leave the semiclassical limit.

The labeling of ergodic and nonergodic states is also worthy of a comment. On many occasions, mainly in the earlier studies, the notations regular and irregular states are used to mean nonergodic and ergodic states, respectively. This notation is probably due to the chaotic (irregular) dynamics of classically ergodic (chaotic) systems and the irregular nodal pattern of ergodic eigenfunctions,[19,22] but by now it should be clear that when we speak of quantum states of ergodic or nonergodic character the inverted notation is actually proper. An (quantum) ergodic system has similar eigenfunctions and less variation in energy level spacing, so that the term "regular" could be appropriate to describe the fact that there are no surprises either in the shape of the eigenstates or in the spacing between adjacent levels. In a nonergodic system, on the other hand, the states look very different in a disorderly way and the energies appear in a random (Poisson) distribution, hence earning the name "irregular" to reflect the independence of one state with respect to a neighboring state. In this work, we will simply not use the terms regular or irregular due to their ambiguous interpretation, and indeed this labeling is no longer very common.

With similarity as the fundamental feature, we have thus seen that previous indicators of quantum ergodicity, obtained using very different approaches, can be viewed as different measures of the similarity/dissimilarity of energy eigenstates, all giving important clues to what would strictly require the investigation of expectation values for a very large number of operators or the globality properties in very many basis sets. If a good measure is designed by which to obtain similarity and globality of energy eigenstates, then this would be the optimal measure for quantum ergodicity.

2.3. Practical Measures of Quantum Ergodicity. In the previous section, we saw that the globality of energy eigenstates and the corresponding similarity between states that are close in energy seem to be the quantum hallmarks of ergodicity. In this section, we will suggest two measures of similarity/globality that should be able to indicate in a qualitative manner whether a system is quantum ergodic or not. We will then use these measures in the following two sections to investigate ergodicity in vibrational systems of two and three dimensions.

Our first measure is based on the investigation of an eigenfunction in configuration space, and an analogous concept could be used to instead investigate the behavior in momentum space, by appropriately Fourier transforming the states. The behavior in configuration space of ergodic states is, as revealed notably by Shnirelman[38,39] and Pechukas,[26] equal to the classical microcanonical density in the semiclassical limit. For finite $\hbar$, we here interpret this to mean that with the proper coarse graining and sufficiently high quantum numbers, each state should not deviate very much from the classical density, nor from the density of neighboring states or the density average of a number of states close in energy. A nonergodic system on the other hand can have states that are trapped in different minima of the potential or that lock kinetic energy to motion in certain directions, causing them to be confined in space. This then, is manifested as wide variations in the coarse grained spatial density between different energy eigenstates and a high degree of deviation from the classical microcanonical density. To be precise, we will define the measure, A_n, to be the L^2 norm of the difference between the coarse grained probability density of ψ_n and the coarse grained reference-density, ϱ, which is either the classical microcanonical density at a suitable energy or the average density obtained from several individual eigenstates energetically close to the state under investigation (and including this state itself). In mathematical terms this means

$$A_n = \frac{\int_V \mathrm{d}\mathbf{x} \left(\int_{\Delta V} \mathrm{d}\mathbf{u}\, |\psi_n(\mathbf{x}+\mathbf{u})|^2 - \int_{\Delta V} \mathrm{d}\mathbf{u}\, \varrho(\mathbf{x}+\mathbf{u})\right)^2}{\int_V \mathrm{d}\mathbf{x} \left(\int_{\Delta V} \mathrm{d}\mathbf{u}\, \varrho(\mathbf{x}+\mathbf{u})\right)^2} \tag{3}$$

where

$$\varrho(\mathbf{x}) = \frac{1}{N}\sum_l |\psi_l(\mathbf{x})|^2 \tag{4}$$

and the sum runs over a small energy interval containing N states (of which the considered state n is one). The coarse graining domain is ΔV, and V is the entire space of dimensionality D. The denominator in eq 3 is the total L^2 norm of the reference density, which provides a kind of normalization to the measure; an ergodic state should yield a value of A_n considerably lower than unity (the exact requirement depends of course on the coarse graining domain size, etc.). As discussed above, the reference density, ϱ, may also be the classical microcanonical density

$$\varrho(\mathbf{x}) \propto (E - V(\mathbf{x}))^{(D-2)/2} \tag{5}$$

which lets us investigate an individual state, without reference

to nearby states but to the price that a classical picture is forced upon a quantum description.

The second measure is obtained in a basis set approach where the expansion coefficients, c_{nj}, of a particular basis are investigated. By choosing a few relevant basis sets and comparing their corresponding outcomes with each other and with the configuration space measure (and possibly also with the corresponding momentum space measure), it should be possible to get a good picture of the ergodic properties of the system. By adding additional basis sets, we can also refine the investigation. An ergodic state will tend to spread more globally and uniformly in most basis sets than would a nonergodic state, which is limited to some particular type of dynamics. A good measure of uniform spread of probability is the Shannon entropy, so that given our basis of interest, $\{j\}$, our precise measure of globality, or spread, in this basis description is taken as

$$S_n = \frac{\sum_j |c_{nj}|^2 \ln(|c_{nj}|^2)}{\sum_j p_j \ln(p_j)} \tag{6}$$

where p_j is the average participation of basis-state no. j

$$p_j = \frac{1}{N}\sum_l |c_{lj}|^2 \tag{7}$$

and the average is again over the N states in a small energy interval containing state n. The denominator in eq 6 provides also in this measure a kind of normalization.

3. Results and Discussion

3.1. Ergodicity in Two-Dimensional Systems: Henon−Heiles and Barbanis. Together with various billiard systems, the two-dimensional system of Henon and Heiles[40] is by far the most well investigated with respect to quantum ergodicity.[15,16,20−23,27,29,30,31] Classically, this system shows an interesting onset of ergodicity as its energy is increased toward the dissociation limit, at which the particle can escape the 2D potential well. Just before dissociation is reached, the portion of phase space occupied by ergodic trajectories is somewhere between 90 and 95%.[40] Apart from the interesting transition toward ergodicity the Henon−Heiles system is of interest as a fairly realistic 2D representation of a real molecular dissociation process, and due to its low dimensionality it is readily handled quantum mechanically.

3.1.1. Classical Trajectories. We will start by looking at a few classical trajectories to get some feeling for the classical ergodic properties of the Henon-Heiles system. The potential defining the system is in Cartesian coordinates given by

$$V(x, y) = \frac{A}{2}(x^2 + y^2) + \lambda\left(x^2 y - \frac{1}{3}y^3\right) \tag{8}$$

i.e., two isotropic harmonic vibrations, coupled by an anharmonic term of strength λ. If plane polar coordinates are used it takes the form

$$V(r, \varphi) = \frac{A}{2}r^2 + \frac{\lambda}{3}r^3 \sin(3\varphi) \tag{9}$$

As can be seen from the polar form, the Henon−Heiles potential has C_3 symmetry, and the three dissociation channels are located at the corners of an equilateral triangle (Figure 1). To avoid the unphysical effect of the potential going to minus infinity beyond the dissociation points, we modify the potential so that any point outside the bound region that has a potential energy less than the dissociation energy ($E_D = A^3/6\lambda^2$) is instead assigned the value E_D. This modification does of course not affect the classical trajectories inside the well but is of practical aid in the quantum calculations to prevent dissociative tunneling. In the rest of this paper, we will refer to this potential simply as the Henon−Heiles potential despite this modification.

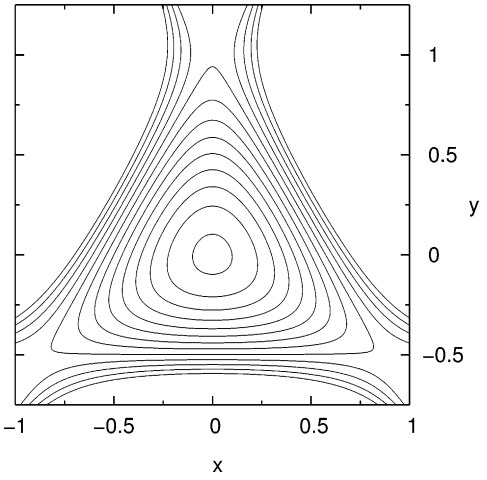

Figure 1. Potential energy surface of the Henon-Heiles system. The lowest contour is 0.005, and the increment between adjacent contours is 0.02. Note that the potential is raised outside the bound region (see text).

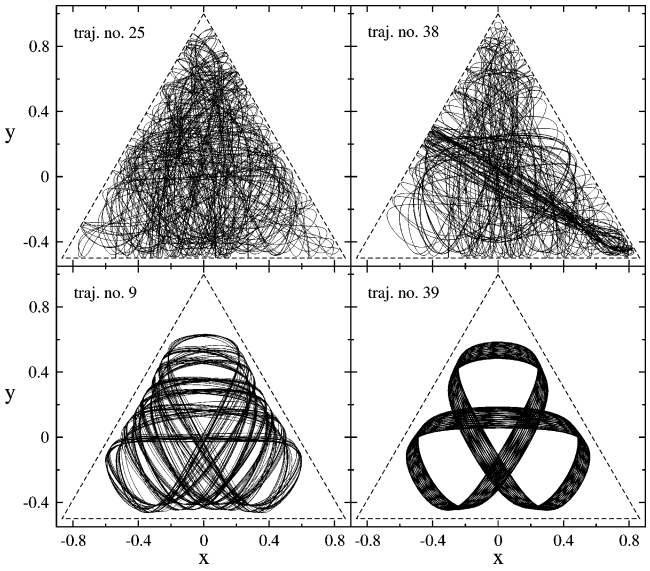

Figure 2. Example of four differently initiated trajectories of the Henon−Heiles system, all at $E = 0.166$ which is very close to dissociation. The sketched triangle is the potential contour for the dissociation energy.

We now turn our interest to Figure 2, where four trajectories (propagated using a Gauss−Radau integrator) with different initial conditions are shown for the case $A = 1$, $\lambda = 1$ at total energy $E = 0.166$ (just below the dissociation energy). The trajectories were initiated randomly from a small region somewhat to the right of the origin with random direction of the velocity vector. We obtain examples of the ergodic type of trajectory (nos. 25 and 38) which are numerous, and we also see typical nonergodic trajectories (nos. 9 and 39), of which we get three or four out of 40 trajectories (but the true ratio between ergodicity and nonergodicity of course demands a

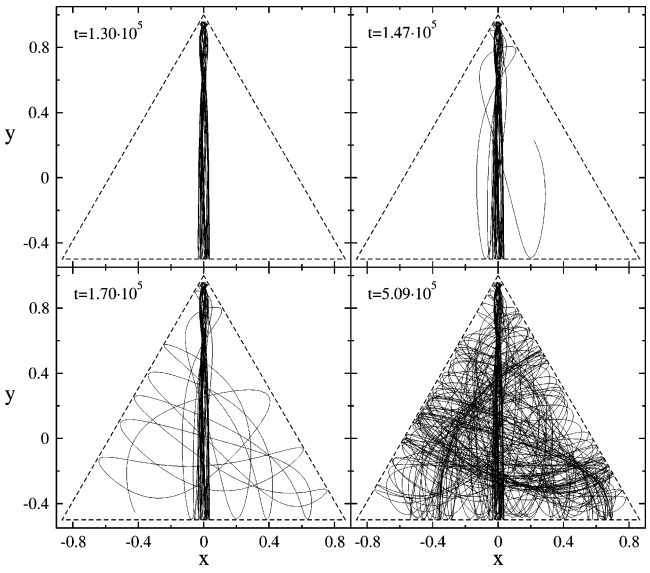

Figure 3. Progress of a trajectory ($E = 0.166$) at four different times. The at first one-dimensional oscillatory motion can be seen to escape this behavior after some time and, thereafter, start to move in an ergodic way. The times are scaled to correspond to the mass 320 000, appearing in the quantum calculations.

proper sampling of the phase space). Strictly speaking, we cannot make precise statements about ergodicity by just looking at a trajectory in configuration space since the definition concerns phase space. However, we can clearly rule out ergodicity in trajectory nos. 9 and 39, whereas trajectory nos. 25 and 38 are really in the ergodic regime as revealed by Poincaré surfaces of section and strongly suggested by their spatial behavior in Figure 2. We also issue a small warning concerning the spatial density indicated by this kind of trajectory plot; since the lines are drawn with constant thickness the eye overestimates the density in regions where the potential is low and the particle moves with higher velocity.

We shall also take a quick glance at a trajectory that at first appears to be clearly nonergodic but after some time actually turns out to be in the ergodic part of phase space. In Figure 3, we see the progress of a trajectory (initiated near the origin and with velocity nearly parallel to the *y* axis) at four different times. At the first instance, we see an almost one-dimensional oscillation which is clearly not ergodic. However, at a slightly longer time (about 20 oscillations in this case), it starts to deviate from its 1D motion, and soon it is clear that the trajectory has begun to behave in an ergodic fashion, much like the first two examples in Figure 2. As a matter of fact, we see the evidence of a similar 1D trajectory in trajectory no. 38, this time turning at the lower right corner and the left border of the triangle. This trajectory did not start in a 1D mode, but entered it after some time and left it after a number of oscillations, making it clear that these 1D modes are in fact a quasi-stable part of the ergodic regime, probably necessary to properly cover also the corners of the triangle shaped accessible region. In contrast, the nonergodic trajectories nos. 9 and 39 of Figure 2 seem to be stable at any time, but it is clear that in practice, at some time a decision about ergodicity must be made, although the fundamental definitions of ergodicity do not concern the time aspect. As a last comment, it should be mentioned that the behavior in Figure 3 is not a numerical artifact. A trajectory propagated at 6 orders of magnitude lower accuracy (in the relative energy conservation) showed no visible deviation from the present trajectory at $t = 1.47 \times 10^5$.

3.1.2. Quantum Mechanical Eigenfunctions. We now want to investigate the quantum mechanical ergodic properties of some two-dimensional systems from the point of view of our discussion about similarity and globality of energy eigenstates, quantified by our suggested measures in section 2.3. We will focus again mainly on the well-known Henon−Heiles system, defined by the 2D Hamiltonian operator (in Cartesian coordinates)

$$\hat{H} = -\frac{\hbar^2}{2\mu}\left(\frac{\partial^2}{\partial x^2} + \frac{\partial^2}{\partial y^2}\right) + V(x, y) \qquad (10)$$

where $V(x, y)$ is the Henon−Heiles potential in eq 8 and pictured in its slightly modified form in Figure 1. Actually, the modification is only slight as far as the bound states are concerned, but the raising of the potential outside the bound region should also make it more physically relevant for quantum dynamics reaching outside the well.

To obtain the energy eigenstates, we diagonalize the Hamiltonian in a basis of product sine-functions (i.e., eigenstates of the 2D particle in a box, where we fit our triangle shaped potential conveniently inside the box), and we treat the states with even and odd parity with respect to reflection in $x = 0$ in separate calculations. The present Cartesian approach is straightforward and has the advantage of an inherent check of the numerical computation by the degeneracy of the energy eigenstates of the *E*-symmetry group, which must be replicated by the two independent even and odd computations. We will now use the same parameters in the potential as we did in the previous section, i.e., $A = 1$, $\lambda = 1$, which is the common case in previous studies, and also the version that Henon and Heiles used in their original work. Furthermore, we set $\hbar = 1$, so that we may interpret our results to be in atomic units, which yields reasonable energies, sizes, etc., from a molecular dynamics point of view. At this time, we also note that the value of the mass, μ, is of no importance to the classical ergodic properties. It merely alters the time scale of the trajectories, not their shape in phase space (in fact in Figure 3, the times appearing are scaled to represent the higher mass that will figure in the quantum calculations). Hence, we may use the mass as a variable which lets us vary the quantum effects and study their impact upon ergodicity (scaling the mass is equivalent to an inverse scaling of $\hbar^2$).

The earlier studies have used the mass 6400 when transformed to our units, and in one case,[30] a mass of 24 400 was used as well. Unfortunately the interest in the Henon-Heiles system seems to have decreased at the time when computer developments made it possible to investigate really high masses and pursue the classical limit. In this work we will investigate the masses 160 000 and 320 000 (corresponding to 88 and 176 amu) for which the number of bound states of even symmetry are 1259 and 2508, respectively. The higher mass Hamiltonian was diagonalized using 19350 product-sine basis functions (for each symmetry), and we will restrict ourselves to this mass when presenting the results. Notably, it turns out that the findings are not very sensitive to which of the two masses that we investigate.

We now apply the two ergodicity measures presented in section 2.3 to the highest bound energy eigenfunctions (even symmetry) of the Henon−Heiles system. The result of the application of the measures is shown in Figure 4. In Figure 4a, we see the L^2 measure of similarity in configuration space, defined by eq 3. The first feature we can see is that the two curves, representing a (coarse grained) comparison of individual

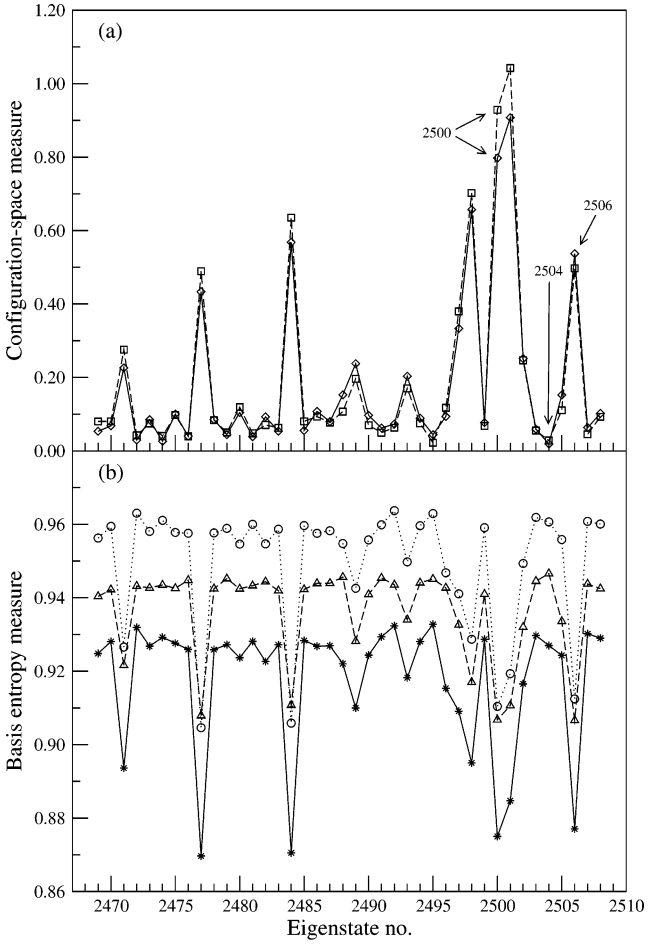

Figure 4. Ergodicity measures for the 40 highest (even parity) states of the Henon−Heiles system. In a, we show the coarse grained difference measure between individual eigenstates and the classical microcanonical density (squares) and the average density of all 40 eigenstates (diamonds). In b, the stars are the entropy measure for the sine basis, the triangles are for the DVR basis in *x*,*y* and circles represent the measure in the momentum DVR basis. Note the correlation between all curves in both parts a and b.

states with the classical microcanonical density (squares) and with the average density of several quantum states (diamonds), look nearly identical. This indicates that the average density of several states (here we have taken the average over all the 40 highest states shown in the figure) must be very close to the classical ergodic microcanonical density (which according to eq 5 is constant throughout the allowed region for a 2D system). On the other hand, individual states show a great variation under this measure which is a clearly nonergodic feature according to our previous discussion about quantum ergodicity and similarity of energy eigenstates close in energy. Clearly, such an important feature of the states as their coarse grained spatial distribution cannot be allowed such wide variations if the system is to be termed quantum ergodic. Also the next analysis, namely the globality measure of spread in expansion coefficients in different basis sets (eq 6), shown in Figure 4b, is seen to vary between the eigenstates. The most striking feature is the very close correlation between all curves (measures) in both parts a and b of the figure, making it probable that the measures indeed are able to qualitatively classify individual states and give an approximate overall picture of the ergodic behavior of the quantum system.

To verify that the peaks shown in Figure 4 indeed detect some sort of nonergodicity, we take a closer look at three eigenstates,

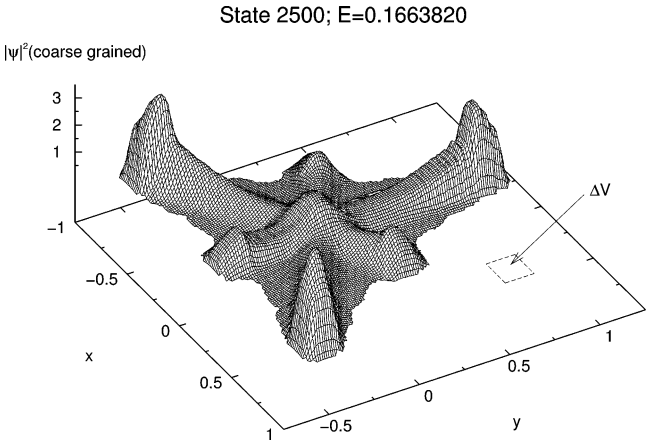

Figure 5. Henon−Heiles; coarse grained probability density for state no. 2500 of even symmetry (coarse graining area is ΔV). This state seems to represent a superposition of the three possible classical one-dimensional oscillations.

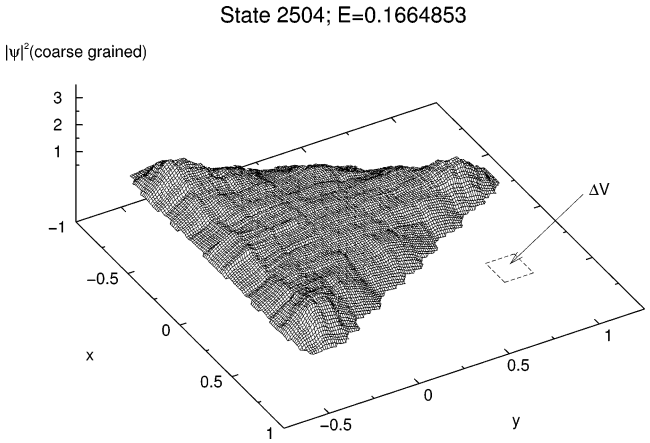

Figure 6. Henon−Heiles; coarse grained probability density for state no. 2504 of even symmetry (coarse graining area is ΔV). This state fills the entire (triangle shaped) accessible region uniformly, hence implying an ergodic behavior.

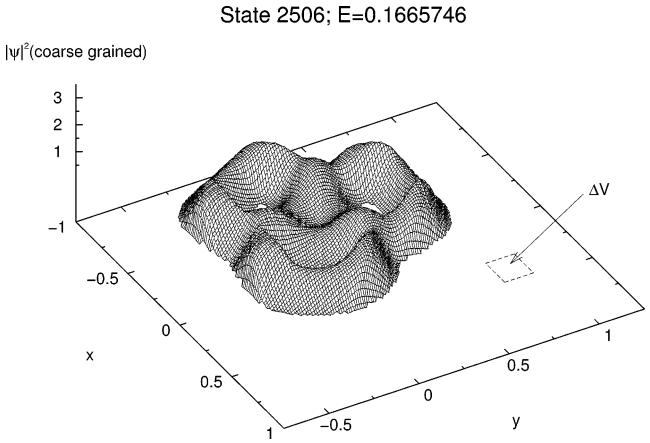

Figure 7. Henon−Heiles; coarse grained probability density for state no. 2506 of even symmetry (coarse graining area is ΔV). Here it clearly looks like we have the quantum version of the classical nonergodic trajectory, which is making a trefoil shaped rotational motion.

namely nos. 2500, 2504, and 2506. The coarse grained probability densities of these three states are shown in Figures 5−7, and the coarse graining region (ΔV of eq 3) which is based on the spatial extension of the vibrational groundstate is also indicated in each figure. The states have nearly the same energy

(exact energies are presented in the figures) but show three completely different types of spatial behavior. State 2504, indicated to be very ergodic by the measures, has uniform coverage of the triangular energetically allowed region which is exactly the result of a microcanonical density in a 2D system. This is what would be demanded of an ergodic state in the semiclassical limit. State 2500 on the other hand, which showed up as a very high nonergodic peak for all measures, is seen to be clearly nonergodic by virtue of its nonuniform spatial distribution which clearly distinguishes it from the ergodic-like state. In fact, state 2500 looks very much like three superposed one-dimensional oscillations of the quasi stable kind shown in classical mechanics if a trajectory is initiated in a proper direction (Figure 3). The difference is that classically this kind of motion persist only for a limited time, but in the case of a quantum energy eigenstate, this behavior will last forever according to eq 2. A third kind of eigenstate is represented by state 2506, which also gives large peaks when we apply our measures. Looking at the coarse grained spatial density, we see a state which does not reach out to the corners of the triangle and has three depleted areas near the central region. We can see that this state should be the quantum equivalent of the classical nonergodic trajectories, pictured in Figure 2 (trajectories labeled 9 and 39), which rotate around the center of the potential in a trefoil shaped pattern. Of our 40 eigenstates, there seem to be six of this kind, with more or less pronounced trefoil behavior. This gives a ratio of 15% (admittedly not very good statistics) to be compared with clearly less than 10% in the classical case. In addition, we have perhaps five states which can be assigned the one-dimensional nonergodic behavior (of which our state 2500 is one of the most pronounced) which has no classical counterpart since these trajectories are unstable classically. The three classes of eigenfunctions (one ergodic and two nonergodic types) were also discussed by Hose et al,[41] and we shall revisit them later in this section.

We have also performed some calculations on an anisotropic version of the Henon−Heiles system, where the two harmonic terms are not equal

$$V(x, y) = \frac{1}{2}(Ax^2 + By^2) + \lambda\left(x^2y - \frac{1}{3}y^3\right) \qquad (11)$$

In order not to lower the dissociation energy too much we made a quite modest change compared with the isotropic case (eq 8) by choosing $A = 1.0$ and $B = 0.95$, while still keeping $\lambda = 1.0$. This breaks the C_3 symmetry and adjusts the upper dissociation channel to $E_D = 0.1429$. Classically, at energies very close to dissociation, we found this system to be more ergodic than the unperturbed Henon−Heiles system (section 3.1.1), and we did not find the kind of nonergodic trajectories seen in Figure 2 (again we did not perform a complete phase space sampling). We then computed the energy eigenstates in the same way as for the Henon−Heiles system above and obtained 1871 even states below the classical dissociation limit. When analyzing these states as above, we found that the behavior was quite close to the one observed for the isotropic case; that is, we saw both clear indications of one-dimensional oscillatory behavior and versions of the classical rotational character (here it looked somewhat more like a circular rotation instead of a trefoil shaped one). Also it was noted that some states which looked mainly ergodic in configuration space (and by the basis measure) seemed to have some superimposed nonergodic part in them, mainly of 1D oscillatory type. Thus, the anisotropic Henon−Heiles system, which showed a higher degree of ergodicity classically, does not have energy eigenstates which indicate a more ergodic behavior. We still see quantum indications of nonergodic rotational character (which was not found classically for the anisotropic case), and also the 1D oscillations are present as before (these are classically unstable for both the anisotropic and isotropic case).

We will also take the opportunity to investigate another famous two-dimensional system according to Barbanis,[42] which has previously also been investigated in connection with quantum ergodicity.[15,16,22] The potential is

$$V(x, y) = \frac{A}{2}(x^2 + y^2) - \lambda x^2 y \qquad (12)$$

with a dissociation energy of $E_D = A^3/8\lambda^2$, which amounts to 0.125 when we choose $A = 1$, $\lambda = 1$. Despite its apparent similarity with the Henon−Heiles system, it turns out that classically the degree of ergodicity just below the dissociation limit is only about 60%,[42] as compared to almost 95% for the Henon−Heiles system near its dissociation limit. In fact, when one considers the spatial appearance of the classical trajectories, it is questionable if any trajectory at all should be referred to as ergodic, since also the trajectories showing the most stochastic behavior lack large spatial regions (which other nonergodic trajectories occupy), hence, implying a quite severe division of phase space.

We again diagonalize the corresponding Hamiltonian and obtain 1388 energy eigenstates of even symmetry up to dissociation. The analysis of the states directly below dissociation yields a clearly more nonergodic impression than for the Henon−Heiles system. We also here get the one-dimensional kind of wave functions (in somewhat larger number than in the Henon-Heiles case), but it is important to note that in the less ergodic classical Barbanis system this kind of 1D trajectories are stable (as they would also be in the Henon−Heiles system at $E = 0.125$). In the Barbanis system, the rotational kind of nonergodicity is more of a mix between a rotation and a 1D motion, and we see evidence of eigenstates having this behavior as well. Moreover, since the "ergodic" states are quite far from occupying the entire phase space, we actually get a generally higher lowest level for our quantum measures, since no state is very close to the average behavior.

We now summarize the situation found in our investigation of quantum ergodicity for our three 2D systems, Henon−Heiles, anisotropic Henon−Heiles, and Barbanis. From our suggested measures and visual inspection of energy eigenstates, it clearly seems that quantum effects promote nonergodicity. This is most profound in the isotropic and anisotropic Henon−Heiles systems which classically are ergodic to a very large extent, whereas the Barbanis system which is clearly more nonergodic classically shows less difference to its likewise very nonergodic quantum behavior. Intuitively, it seems reasonable that quantum mechanics should somehow support periodic motions due to the wave nature of the solutions benefiting from the possibility of constructive interference.

Amplification of nonstable classical periodic orbits in quantum mechanics was indeed demonstrated by Heller[28] for the case of a stadium billiard. The unstable classical orbits showed up as clearly visible scars of high amplitude in the energy eigenstates. It would seem as if the Henon−Heiles eigenfunctions which display superimposed one-dimensional (classically unstable) oscillatory motion are precisely a scarring phenomena. Also the fact that we seem to have a somewhat larger proportion of states corresponding to the true classical periodic nonergodicity (the rotational trefoil shaped motion) could then be motivated by similar arguments of quantum mechanics favoring

a periodic behavior. Especially, the anisotropic Henon-Heiles system where this nonergodicity is more or less absent classically, does still have about as many quantum "trefoil states" as the isotropic version.

We then expect that due to quantum effects we cannot hope in general to reach the extent of ergodicity shown for the classical system unless the mass is very large. How large then? Since it is our belief that the correspondence principle will eventually force any quantum system to mimic the classical features, the most interesting question is whether it happens at chemically relevant masses. If we interpret our 2D results as atomic units, we have a particle of mass 176 amu, corresponding to the sixth period in the table of elements, and which is confined in a two-dimensional region with a side on the order of 1 Å at an energy in the vicinity of 4 eV. These numbers would lead us to suspect that classical mechanics is a rather good approximation, but still we have clear quantum effects in terms of nonergodic behavior. We also note that, when calculations were performed with half the mass for the Henon−Heiles system, no qualitative change of the picture could be seen. Instead it would be interesting to increase the mass to approach the classical limit, but this would demand a more elaborate approach for the diagonalization procedure and is outside the scope of this work.

One possible explanation of the fact that we, despite the high mass, have quantum effects causing nonergodicity is that the mixing of the dynamics predominately take place near the classical turning points where the kinetic energy is low. This corresponds to long de Broglie wavelengths and thus sizable quantum effects even for high masses. Classically, it is probably the upper part of the potential that promotes ergodic behavior, as mentioned already in the original work by Henon and Heiles.[40] This is to be expected since the coupling term goes as r^3, and indeed, we see for example stable classical nonergodic 1D oscillations at lower energies when the trajectories do not reach as far out in the potential well. Thus, one could suspect that the quantum effects causing nonergodicity would disappear and allow an approach to the classical behavior at such high masses (or small values of $\hbar$, etc.) that the eigenfunctions may represent an advanced dynamics (many nodes and rich structure) even near the classical turning points.

3.1.3. Quantum Wave Packet Dynamics. In this section, it is shown how the nonergodic character of the energy eigenstates of the Henon−Heiles system is reflected in the quantum dynamical wave packet propagation. We then want to solve the time-dependent Schrödinger equation

$$i\hbar \frac{\partial \Psi(x, y, t)}{\partial t} = \hat{H}\Psi(x, y, t) \tag{13}$$

where $\hat{H}$ is defined by eqs 8 and 10, and we set $\mu = 320\,000$. We have added a smooth repulsive potential barrier (which goes such as y^5) beyond the dissociation limit in the upper dissociation channel of the Henon−Heiles potential, to reflect the dissociative components of the wave packet rather than letting them escape. In the two lower dissociation channels, however, we allow dissociation and hence utilize absorbing boundaries[43] to allow a finite grid size. The grid where we propagate our wave packet corresponds to $-1.60 \le x \le 1.60$ and $-1.35 \le y \le 1.85$ with 840 grid points in both the x and y direction. The propagation is done via the split operator method,[44] with the kinetic part of the propagator evaluated by Fourier transformation of the wave function.[45] The time step is 2.5, and we perform the damping action of the absorbing boundaries at each time step.

For this investigation, the initial state at $t = 0$ is taken to be of Gaussian shape and placed at the origin, where the Henon−Heiles potential has its minimum. Thus

$$\Psi(x, y, 0) = \left(\frac{1}{2\pi\sigma_x^2}\right)^{1/4} \exp[-ik_x x - x^2/4\sigma_x^2] \times \left(\frac{1}{2\pi\sigma_y^2}\right)^{1/4} \exp[-ik_y y - y^2/4\sigma_y^2] \tag{14}$$

where $\sigma_x = \sigma_y = 0.0636$, giving a narrow initial wave packet. The wavenumbers (k_x, k_y) are related to the momenta by $p_x = \hbar k_x$ and $p_y = \hbar k_y$, and we vary these to obtain different directions of the momenta of the initial wave packet. The energy expectation value of the wave function will be 0.16, and with the chosen values of σ_x,σ_y, we get an energy dispersion of 0.0087. Remembering that the dissociation threshold is 0.1667, we will clearly have the possibility of some dissociation.

We shall propagate three wave packets to an end-time of $t = 2.0 \times 10^6$ (about 560 harmonic oscillations or 50 ps if interpreted as atomic units), and they will differ by their initial angle of the vector (p_x, p_y) relative to the y axis. In case (i), this angle is very small (1.4°), making the initial movement of the wave packet nearly parallel to the y axis. For cases (ii) and (iii), we start with larger angles (16.7° and 26.6°, respectively). We are interested in the time averaged behavior of the wave packet at long times, so we form the quantity $\langle|\Psi|^2\rangle$ which is the average of the spatial density $|\Psi(t)|^2$ from $t = 1.8 \times 10^6$ to the end time $t = 2.0 \times 10^6$.

The time average, $\langle|\Psi|^2\rangle$, of the wave packets is shown in Figures 8−10, for cases (i), (ii), and (iii), respectively. We clearly see that the nonergodic features of the quantum mechanical Henon−Heiles system discussed in the previous section are reflected in the dynamics, since the average behavior of the three different initial conditions at long times show completely different properties. As could be suspected, case (i), which had its initial momentum nearly parallel to the y axis, has picked up much of the one-dimensional oscillatory character via eigenstates of the type shown in Figure 5. This then means that such a wave packet will evolve in time in a manner that is always affected by this nonergodicity, as is so clearly shown in Figure 8. At the maximum time, $t = 2.0 \times 10^6$, this particular wave packet had a norm of 0.897, which means that about 10% of it has escaped through the two open dissociation channels at

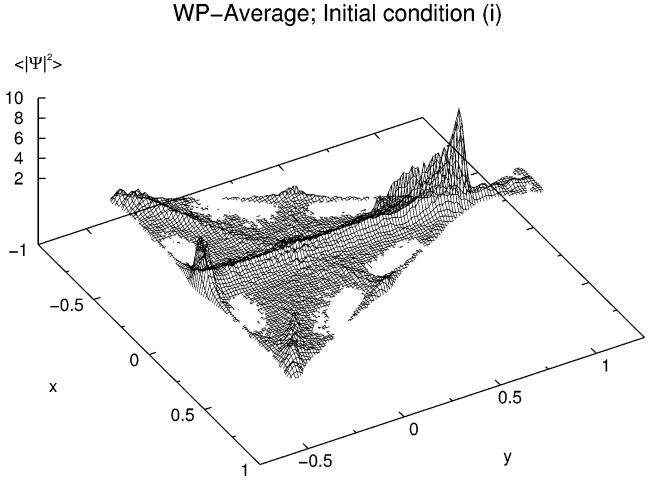

Figure 8. Henon−Heiles; time average of the spatial probability density for case (i), where the initial wave packet at the origin was launched at an angle of 1.4° relative the y axis and with total energy $E = 0.16$. The cutoff on the z axis is at 0.3.

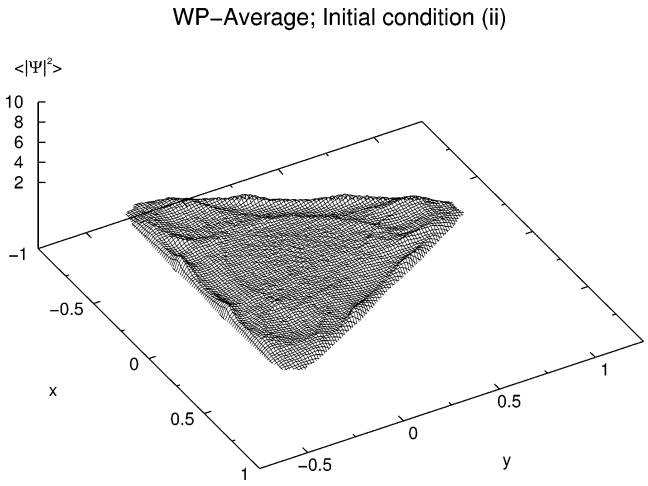

Figure 9. Henon−Heiles; time average of the spatial probability density for case (ii), where the initial wave packet at the origin was launched at an angle of 16.7° relative the *y* axis and with total energy $E = 0.16$. The cutoff on the *z* axis is at 0.3.

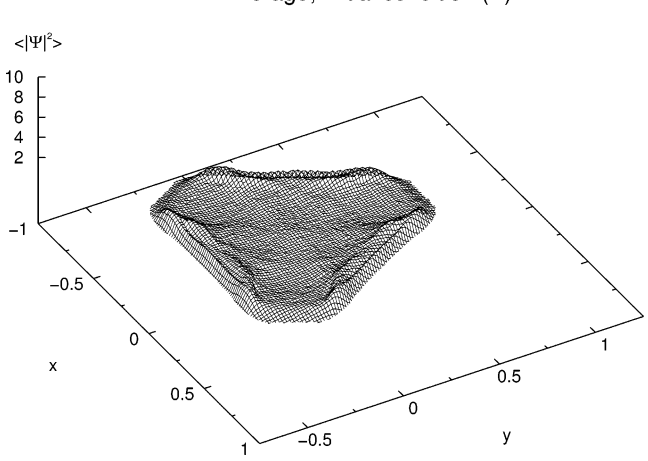

Figure 10. Henon-Heiles; time average of the spatial probability density for case (iii), where the initial wave packet at the origin was launched at an angle of 26.6° relative the *y* axis and with total energy $E = 0.16$. The cutoff on the *z* axis is at 0.3.

the lower corners of the potential surface. Case (ii), which was initiated in a direction of about 17° relative to the *y* axis, shows instead a quite even spread of spatial probability, indicating a more ergodic behavior. Comparing the wave packet average in Figure 9 with the ergodic type of wave function, exemplified by Figure 6, it seems likely that we have a large proportion of such eigenstates in the wave packet expansion. The norm of the wave packet at the maximum time was 0.879, so the high energy components have found their way out from the bound region. In the last example, case (iii), we start with a still larger angle (27°) with respect to the *y* axis and with this choice it turns out, as indicated by Figure 10, that we to a large extent get stuck in the trefoil-shaped rotational behavior supported by eigenfunctions of the shape shown in Figure 7. This is the type of nonergodicity presented also by classical mechanics at high energies as two of the trajectories in Figure 2 demonstrate. This behavior of the wave packet also prevents a proper dissociation, and the norm of the wave packet at $t = 2.0 \times 10^6$ is as high as 0.940.

To summarize we have seen different types of long time behavior of the wave packet dynamics depending on initial conditions, which is the very essence of nonergodicity. We also understand how the ergodic properties of the eigenfunctions have a direct and profound impact on the quantum dynamics of the system.

3.2. Three-Dimensional System: Vibration of NO_2 at Zero Total Angular Momentum. *3.2.1. Quantum Mechanical Representation.* After discussing two-dimensional model systems in the previous section, we now turn to a more realistic case in three dimensions, namely the high lying vibrational states of the NO_2 molecule in its adiabatic electronic groundstate as given by a slightly modified[46−48] version of the ab initio surface of Leonardi, Petrongolo, Hirsch, and Buenker.[49] We restrict ourselves to the case of zero total angular momentum, $J = 0$, for which the Hamiltonian of a triatomic molecule in hyperspherical coordinates takes the following form[47,48]

$$\hat{H} = -\frac{\hbar^2}{2\mu}\left\{\frac{\partial^2}{\partial\rho^2} + \frac{16}{\rho^2}\hat{L}^2(\theta,\phi)\right\} + \frac{15\hbar^2}{8\mu\rho^2} + V(\rho,\theta,\phi) \quad (15)$$

where $\hat{L}^2(\theta,\phi)$ is the grand angular operator

$$\hat{L}^2(\theta,\phi) = -\left[\frac{1}{\sin(\theta)}\frac{\partial}{\partial\theta}\sin(\theta)\frac{\partial}{\partial\theta} + \frac{1}{4\sin^2(\theta/2)}\frac{\partial^2}{\partial\phi^2}\right] \quad (16)$$

μ is the reduced mass

$$\mu = (m_N m_O m_{O'}/M)^{1/2} \quad (17)$$

and M is the total mass of the molecule

$$M = (m_N + m_O + m_{O'}) \quad (18)$$

The volume element is given by

$$d\tau = \frac{1}{32}d\rho\,\sin(\theta)d\theta d\phi \quad (19)$$

These hyperspherical coordinates[47,48] are such that $0 \le \theta \le \pi$, $0 \le \phi \le 2\pi$, and for the present potential the ρ range 3.0 bohr $\le \rho \le$ 6.8 bohr is suitable when we limit our calculations to bound states. Furthermore, since we have the symmetry of two identical oxygen atoms, a ϕ range of 0 to π will suffice, and we may perform the calculations for even and odd states with respect to ϕ independently.

We work in a mixed DVR−FBR basis[47,48] where the hyperradius, ρ, is described as a DVR-grid, $|\rho_\alpha\rangle$, and (for each discrete value of the hyperradius) the hyperangles (θ, ϕ) are treated in a basis of the (analytical) eigenstates, $|jm\rangle$, of the grand angular operator $\hat{L}^2$. In this way, the application of the $\hat{L}^2$ part of the Hamiltonian is only a multiplication with the corresponding eigenvalue, and the derivatives with respect to ρ are computed via FFT. When it comes to the potential part, we transform the $|jm\rangle$ basis to a grid representation, $|\theta_\beta\phi_\gamma\rangle$, within a global quadrature scheme, and after multiplication with the potential, we transform back to the mixed DVR−FBR basis.

The basis used is $N_\rho \times N_\theta \times N_\phi = 168 \times 115 \times 105 =$ 2 028 600, which means that a direct diagonalization is out of the question. Since we will only need a few states near dissociation, we use instead the same method as in ref 48, i.e., a restarted spectral filtering method, where repeated application of the Hamiltonian is used to generate a sharp energy envelope (the spectral filter). By restarting the sequence with sharper and sharper filters, a pure state may be obtained. The computational efficiency of this method is not very high, but it gives access to individual states (and corresponding energies) and by continuing the iterations it is easy to adjust to the requested accuracy. We used the method to calculate the 20 highest

TABLE 1: Energies[a] for the NO_2 Vibrational States Obtained by the Restarted Spectral Filtering Procedure

number	*E*/eV	number	*E*/eV
1815	3.334908	1825	3.339759
1816	3.335418	1826	3.340283
1817	3.335916	1827	3.341007
1818[b]	3.336697	1828	3.341313
1819	3.336955	1829	3.341673
1820	3.337063	1830	3.342051
1821	3.337919	1831	3.342385
1822	3.338610	1832	3.342979
1823	3.339191	1833	3.343626
1824	3.339299	1834	3.343663

[a] All digits shown are significant. [b] False state supported by the artificial potential well (see text).

vibrational states of even parity, directly below the quantum mechanical dissociation limit. The energies of the obtained states are presented in Table 1. The numbering of the levels is according to ref 47, where all bound energy eigenvalues were calculated. In Table 1, one of the states, no. 1818, was actually found (by the ergodicity criteria) to be an artificial state due to a flaw in the potential energy surface. Further investigations led to the conclusion that this state lives in an unphysical well at θ, ϕ, close to π (corresponding to very small distance between the oxygen atoms). Since this well is clearly separated from the interesting part of the potential, it is easy to lift the well to remedy the deficiency. We do not know if this problem with the potential is original,[49] or if it is due to the modifications,[46] but we issue a warning that a small part of previously calculated levels of this potential may be artificial.

3.2.2. Ergodic Analysis. For the ergodic analysis of NO_2, we use the two kinds of measure discussed in section 2.3 and tested successfully on the Henon−Heiles system in section 3.1.2. We point out again that this approach gave good indications (and good mutual correlation) of the ergodic/nonergodic behavior suggested by visual inspection of the eigenstates in configuration space for all three 2D systems investigated above. Thus, we have good hope that it will now give good indications of ergodic character also for the NO_2 system, where visual inspection is a cumbersome procedure due to the three-dimensional nature of the problem.

First we investigate the spatial behavior of eigenfunctions through a comparison of individual probability distributions with the averaged distribution of several eigenstates and the classical microcanonical density, respectively. As in the case of the Henon−Heiles system, the measure is the L^2 norm of the coarse grained difference, and care has been taken to somewhat adapt the coarse graining volume to the local wavelength. Concerning the classical microcanonical density, it was obtained for each hyperspherical grid point as described in the Appendix. The result is that the classical microcanonical density at $E = 3.2263$ eV (the classical dissociation limit) is very similar to the average density of our 19 states as indicated by Figure 11, where we have integrated out the hyperangles and show the probability density as function of the hyperradius (no coarse graining is performed in this figure). Also the density of two individual states are seen to be quite similar to the quantum and classical reference densities. In Figure 12a, we see the results for the 20 (19) highest bound states of NO_2. It is seen that the measure is not varying nearly as much as in the Henon−Heiles case (Figure 4a), suggesting a mainly ergodic behavior, at least with respect to configuration space. The state no. 1821 is somewhat higher than the rest, so we keep an extra eye on it when applying the next analysis method (but we note that this state at least seems to behave reasonably with respect to its probability density in ρ according to Figure 11).

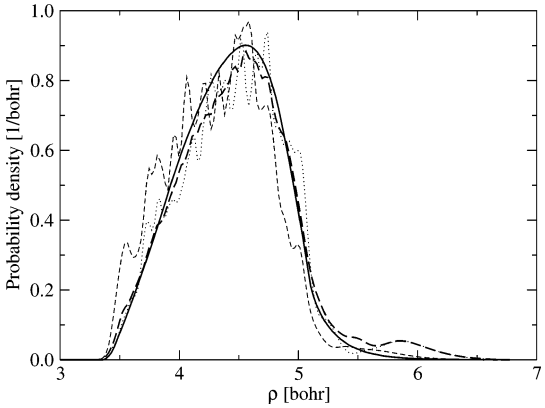

Figure 11. NO_2; probability density in the hyperradius ρ. The full line is the classical microcanonical density at an energy precisely below the classical dissociation limit, which can be seen to agree very well with the average quantum density represented by the fat dashed line. The short-dashed and dotted lines represent the individual states nos. 1821 and 1828, respectively.

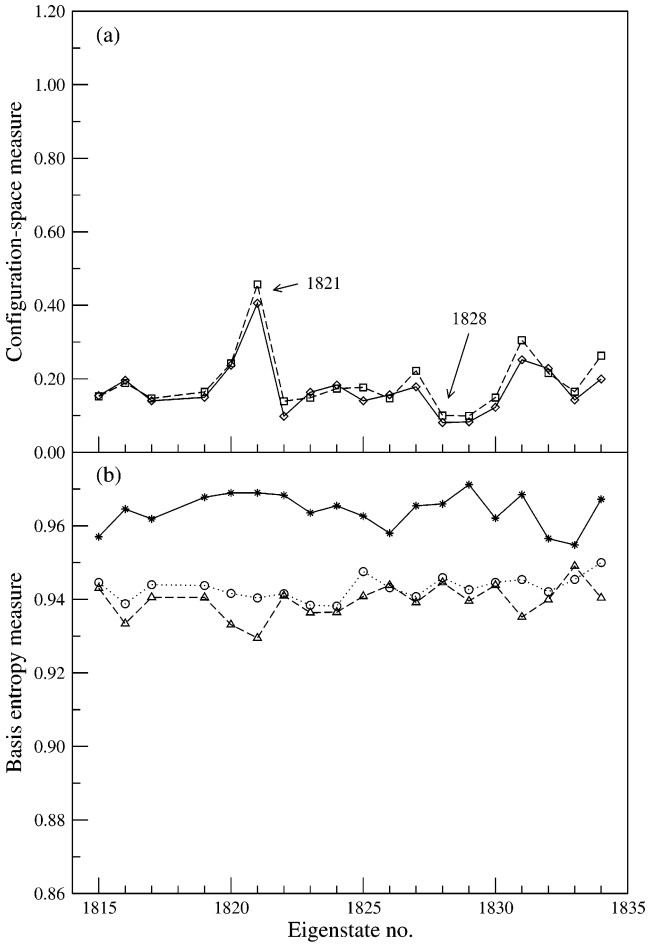

Figure 12. Ergodicity measures for the 19 highest (of even parity) vibrational states of NO_2 at $J = 0$ (the artificial state no. 1818 is deleted). In a, we show the coarse grained difference measure between individual eigenstates and the classical microcanonical density (squares) and the average density of all 19 eigenstates (diamonds). In b, the stars are the entropy measure for the FBR basis, the triangles represent the DVR basis, and the circles correspond to the measure in the mixed DVR−FBR basis.

Now we apply the basis-entropy criterion to the same eigenstates. We have two natural basis sets to investigate,

namely the FBR basis (eigenstates of $\hat{L}^2$ in θ, ϕ, and Fourier states in ρ) and the DVR basis (hyperspherical configuration space) described above. Also, we will include the mixed DVR-(ρ)-FBR(θ,ϕ) basis in which the wave function is normally stored during the calculations. The result of the measure is shown in Figure 12b, where we see that there is hardly any correlations between the curves, nor with the measure in Figure 12a. This further supports the indications that the states of NO_2 are indeed to a large part ergodic near the dissociation limit. This is in accord with a previously performed eigenvalue analysis,[47] where the nearest neighbor spacing distribution was calculated (for the 218 highest levels) showing the level repulsion to conform to Wigner statistics rather than to the nonergodic Poisson distribution.

4. Conclusions

We have investigated the concept of quantum ergodicity with emphasis on its connection to the behavior of the energy eigenstates and, therefore, also the qualitative impact on the quantum dynamics of the system. The following points are of special interest in this study.

(1) By taking the standpoint that a fundamental characteristic of an ergodic quantum dynamical motion is the similarity of eigenfunctions close in energy, we arrive at a concept of quantum ergodicity closely adhering to the classical meaning. It naturally include previous studies as different ways of measuring the similarity of eigenfunctions. Similarity means that all of the energy eigenstates are global and that all states in a small energy interval will have equal statistical weight in the expansion of an arbitrary (initial) state.

(2) Quantum effects are seen to amplify nonergodic behavior. By investigation of the Henon−Heiles system near dissociation, we observe a fraction of clearly nonergodic eigenfunctions of about 25%. This is to be compared to less than 10% nonergodic portion of the classical phase space. In particular eigenfunctions of one-dimensional oscillatory character are especially profound. Such oscillations are not stable classically but can prevail for quite long times.

(3) The nonergodicity of the quantum Henon−Heiles system described above persists even to the highest masses that we were able to treat numerically, and actually the degree of nonergodicity was approximately the same when two different masses (factor of 2) were investigated. One possible explanation is that the classical mixing of phase space mostly takes place near the turning points, where the kinetic energy is so low that sizable quantum effects are present even for very high masses.

(4) Points 2 and 3 above are also qualitatively valid for the anisotropic (perturbed) Henon−Heiles system and the Barbanis system. For the anisotropic Henon−Heiles system, the difference between classical and quantum mechanics is even more pronounced, since this system has a higher degree of ergodicity classically, whereas the Barbanis system which is quite nonergodic classically gives better correspondence to the likewise nonergodic behavior of the eigenfunctions.

(5) A way to partially automate the analysis of ergodic behavior is suggested by our two measures, based on globality in terms of basis functions and coarse grained similarity in configuration space, respectively. These measures are easy to apply, and by investigating their correlation, it seems that one can get a reasonably accurate indication of ergodicity. By including additional basis sets in the analysis the picture can be gradually refined.

(6) As expected, it is seen that the different properties of the energy eigenfunctions of the Henon−Heiles system has a direct impact on the quantum dynamics. The time propagation of wave packets show a clearly nonergodic behavior, and the time average of the spatial density may conform to any of the different types of eigenfunctions depending on initial conditions.

(7) By applying our measures to the vibrational states of NO_2 near dissociation we showed that the eigenstates present a high degree of similarity implying an ergodic behavior. This is in accord with previously performed energy level statistics (see, e.g., ref 47), which is the standard way to get an indication of the ergodic nature of a system. The measure is also more convenient than the common investigations of the nodal behavior of a wave function, since this becomes a cumbersome task in more than two dimensions.

Acknowledgment. This paper is dedicated to the late professor Gert Due Billing, whose scientific contributions to the field of molecular quantum dynamics will continue to inspire us. The research presented in this work was supported by the Swedish Research Council (VR).

Appendix

The quantum mechanical probability density is obtained on the hyperspherical grid (ρ_α,θ_β,ϕ_γ) by squaring the corresponding value of the $J = 0$ wave function and including the volume element and quadrature weights. To assign classical probabilities to these grid points we proceed in two steps as follows.

First, a volume is assigned to each hyperspherical grid point by enclosing it by a box centered on the grid point. Together the boxes fill all space between the grid points. Each box is spanned by three vectors, defined by four corners of the box. A coordinate transformation to internal coordinates is performed for each of the four corners using the equations[50]

$$\begin{cases} r_{\mathrm{NO}}{}^2 = \frac{1}{2} d_{\mathrm{O}'}{}^2 \rho^2 \left[1 + \sin(\theta/2) \cos(\phi + \chi_{\mathrm{NO}'})\right] \\ r_{\mathrm{OO}'}{}^2 = \frac{1}{2} d_{\mathrm{N}}{}^2 \rho^2 \left[1 + \sin(\theta/2) \cos(\phi)\right] \\ r_{\mathrm{NO}'}{}^2 = \frac{1}{2} d_{\mathrm{O}}{}^2 \rho^2 \left[1 + \sin(\theta/2) \cos(\phi - \chi_{\mathrm{NO}})\right] \end{cases}$$

where the channel angles are given by $\chi_{\mathrm{NO}} = 2 \tan^{-1}(m_{\mathrm{O}'}/\mu)$ and $\chi_{\mathrm{NO}'} = 2 \tan^{-1}(m_{\mathrm{O}}/\mu)$, and the scaling parameter for each species is $d_k{}^2 = (m_k/\mu)(1 - m_k/M)$ with μ and M defined in eqs 17 and 18. The four points now obtained in internal coordinates define three vectors (**a**,**b**,**c**) in this space. It is assumed that the volume corresponding to each box in the hyperspherical coordinates is proportional to $V = |(\mathbf{a} \times \mathbf{b})\cdot\mathbf{c}|$, which would be exact for an infinitesimally small box.

Second, we transform each grid point to internal coordinates and calculate the corresponding angular momentum resolved classical density[51]

$$w \propto r_{\mathrm{NO}}{}^2 r_{\mathrm{NO}'}{}^2 \sin(\eta)(I_1 I_2 I_3)^{-1/2}[E - \epsilon_r - V(r_{\mathrm{NO}}, r_{\mathrm{NO}'}, \eta)]^{1/2}$$

where η is the O−N−O′ angle, I_1, I_2, I_3 are the principal moments of inertia, and the rotational energy, ϵ_r, is zero for $J = 0$. Finally, the classical weight $\varrho = Vw$ is assigned to each hyperspherical grid point. The weights for all grid points are summed and normalized to unity, giving probabilities for each grid point that are directly comparable with the quantum mechanical probability obtained from the $J = 0$ wave function. Special care was taken in defining the boxes at the edges of the hyperspherical grid.

References and Notes

(1) Marcus, R. A.; Rice, O. K. *J. Phys. Chem.* **1951**, *55*, 894.
(2) Baer, T.; Hase, W. L. *Unimolecular Reaction Dynamics*; Oxford: New York, 1996.
(3) Slater, N. B. *Theory of Unimolecular Reactions*; Methuen: London, 1959.
(4) Šolc, M. *Mol. Phys.* **1967**, *12*, 101. Slater, N. B. *Mol. Phys.* **1967**, *12*, 107. Šolc, M. *Chem. Phys. Lett.* **1967**, *1*, 160.
(5) Gray, S. K.; Rice, S. A.; Davis J. *J. Phys. Chem.* **1986**, *90*, 3470.
(6) Nordholm S. *Chem. Phys.* **1989**, *137*, 109.
(7) Leitner, D. M.; Wolynes P. G. *Chem. Phys. Lett.* **1997**, *280*, 411.
(8) Nordholm, S.; Bäck, A. *Phys. Chem. Chem. Phys.* **2001**, *3*, 2289.
(9) Shapiro, M.; Brumer, P. *Principles of the Quantum Control of Molecular Processes*; Wiley: Hoboken, NJ, 2003.
(10) von Neumann, J. *Z. Phys.* **1929**, *57*, 30 (in German).
(11) Jancel, R. *Foundations of Classical and Quantum Statistical Mechanics*; Pergamon: London, 1969.
(12) Porter, C. E. *Statistical Theories of Spectra: Fluctuations*; Academic: New York, 1965.
(13) Percival, I. C. *J. Phys. B* **1973**, *6*, L229.
(14) Pomphrey, N. *J. Phys. B* **1974**, *7*, 1909.
(15) Nordholm, S.; Rice, S. A. *J. Chem. Phys.* **1974**, *61*, 203. Nordholm, S.; Rice, S. A. *J. Chem. Phys.* **1974**, *61*, 768.
(16) Nordholm, S.; Rice, S. A. *J. Chem. Phys.* **1975**, *62*, 157.
(17) Berry, M. V. *J. Phys. A* **1977**, *10*, 2083.
(18) Wigner, E. *Phys. Rev.* **1932**, *40*, 749.
(19) McDonald, S. W.; Kaufman, A. N. *Phys. Rev. Lett.* **1979**, *42*, 1189.
(20) Heller, E. J. *Chem. Phys. Lett.* **1979**, *60*, 338.
(21) Kosloff, R.; Rice, S. A. *Chem. Phys. Lett.* **1980**, *69*, 209.
(22) Stratt, R. M.; Handy, N. C.; Miller, W. H. *J. Chem. Phys.* **1979**, *71*, 3311.
(23) Hutchinson, J. S.; Wyatt, R. E. *Chem. Phys. Lett.* **1980**, *72*, 378.
(24) Kay, K. G. *J. Chem. Phys.* **1980**, *72*, 5955.
(25) Brumer, P.; Shapiro, M. *Chem. Phys. Lett.* **1980**, *72*, 528. Davis, M. J.; Stechel, E. B.; Heller, E. J. *Chem. Phys. Lett.* **1980**, *76*, 21. Shapiro, M.; Brumer, P. *Chem. Phys. Lett.* **1982**, *90*, 481. Heller, E. J.; Stechel, E. B. *Chem. Phys. Lett.* **1982**, *90*, 484.
(26) Pechukas, P. *Phys. Rev. Lett.* **1983**, *51*, 943.
(27) Feit, M. D.; Fleck, J. A., Jr. *J. Chem. Phys.* **1984**, *80*, 2578.
(28) Heller, E. J. *Phys. Rev. Lett.* **1984**, *53*, 1515.
(29) Peres, A. *Phys. Rev. A* **1984**, *30*, 504. Feingold, M.; Moiseyev, N.; Peres, A. *Phys. Rev. A* **1984**, *30*, 509. Feingold, M.; Moiseyev, N.; Peres, A. *Chem. Phys. Lett.* **1985**, *117*, 344.
(30) Kay, K. G. *J. Chem. Phys.* **1983**, *79*, 3026. Ramachandran, B.; Kay, K. G. *J. Chem. Phys.* **1985**, *83*, 6316. Ramachandran, B.; Kay, K. G. *J. Chem. Phys.* **1987**, *86*, 4628.
(31) Billing, G. D.; Jolicard, G. *Chem. Phys. Lett.* **1989**, *155*, 521.
(32) Benet, L.; Seligman, T. H.; Weidenmüller, H. A. *Phys. Rev. Lett.* **1993**, *71*, 529.
(33) De Polavieja, G. G.; Borondo, F.; Benito, R. M. *Int. J. Quantum Chem.* **1994**, *51*, 555.
(34) Kaplan, L.; Heller, E. J. *Physica D* **1998**, *121*, 1. Zelditch, S. *Physica D* **1998**, *121*, 19.
(35) Aurich, R.; Bäcker, A.; Schubert, R.; Taglieber, M. *Physica D* **1999**, *129*, 1.
(36) Birkhof, G. D. *Proc. Natl. Acad. Sci. U.S.A.* **1931**, *17*, 650. Birkhof, G. D. *Proc. Natl. Acad. Sci. U.S.A.* **1931**, *17*, 656.
(37) Bäck, A. Licentiate Thesis, Göteborg University, Göteborg, Sweden, 2002.
(38) Shnirelman, A. I. *Usp. Mat. Nauk* **1974**, *29*, 181 (in Russian).
(39) Shnirelman, A. I. In *KAM Theory and Semiclassical Approximations to Eigenfunctions*; Lazutkin, V. F., Ed.; Springer: Berlin, 1993; p 313.
(40) Henon, M.; Heiles, C. *Astron. J.* **1964**, *69*, 73.
(41) Hose, G.; Taylor, H. S.; Bai, Y. Y. *J. Chem. Phys.* **1984**, *80*, 4363.
(42) Barbanis, B. *Astron. J.* **1966**, *71*, 415.
(43) Vibók, Á.; Balint-Kurti, G. G. *J. Phys. Chem.* **1992**, *96*, 8712.
(44) Feit, M. D.; Fleck, J. A.; Steiger, A. *J. Comput. Phys.* **1982**, *47*, 412.
(45) Kosloff, D.; Kosloff, R. *J. Comput. Phys.* **1983**, *52*, 35.
(46) Salzgeber, R. F.; Mandelshtam, V.; Schlier, Ch; Taylor, H. S. *J. Chem. Phys.* **1998**, *109*, 937.
(47) Yu, H.-G.; Nyman, G. *J. Chem. Phys.* **1999**, *110*, 11133.
(48) Bäck, A. *J. Chem. Phys.* **2002**, *117*, 8314.
(49) Leonardi, E.; Petrongolo, C.; Hirsch, G.; Buenker, R. J. *J. Chem. Phys.* **1996**, *105*, 9051.
(50) Varandas, A. J. C.; Yu, H.-G. *J. Chem. Soc., Faraday Trans.* **1997**, *93*, 819; **1997**, *93*, 3599 (corrigendum).
(51) Nyman, G.; Nordholm, S.; Schranz, H. W. *J. Chem. Phys.* **1990**, *93*, 6767.